Since similar decreases in δ and ΔE_Q reported for the FePc derivatives are observed for a wide range of iron(II)–macrocyclic complexes[10,13,14,36] for which the relative orbital energies and hence bonding characteristics should vary, we shall turn our attention to some structural data for these compounds.

In all cases for which structural data are available,[37–40] carbonylation results in a longer Fe–L(axial) bond length, but the Fe–C(O) bond distance is sufficiently short to cause a decrease in the sum of the axial bond lengths relative to the bis(L) adducts. Such a shortening of the mean axial bonds will increase the electron density near iron along the z axis and result in a decrease in ΔE_Q. If this electron density has appreciable s character, δ will also decrease. We suggest that these overall structural changes, irrespective of the σ- and π-bonding characteristics of the ligands, dominate the changes in Mössbauer parameters.

No structural data are available for dicarbonyl complexes nor has the sign of the EFG been determined in such a species (although it is probably positive). This limits the present discussion of $FePc(CO)_2$ which gives one of the lowest $|\Delta E_Q|$ values yet reported for a (phthalocyaninato)iron(II) complex. It is tempting to suggest that this results from a significant demand on the Pc π system, but further analysis awaits a detailed investigation of $Fe(TPP)(CO)_2$.

Acknowledgment. The authors wish to thank the National Research Council of Italy and the Natural Sciences and Engineering Research Council of Canada for support of this work and the Scuola Normale Superiore of Pisa for a postdoctoral fellowship to G.P.

Registry No. FePc(CO)(DEA), 80720-96-3; FePc(CO)(py), 61395-36-6; FePc(CO)(pip), 68949-32-6; FePc(CO)(HMPT), 80737-35-5; $FePc(CO)(OPPh_3)$, 80737-36-6; $FePc(CO)_2$, 80737-37-7; $FePc(CO)(H_2O)$, 74335-17-4; $FePc(CO)(Me_2SO)$, 58384-96-6; FePc(CO)(DMF), 71744-40-6; FePc(CO)(MeOH), 74325-92-1; FePc(CO)(THT), 80737-38-8; $FePc(CO)(n\text{-}Pr\text{-}NH_2)$, 71851-41-7; $FePc(CO)(NH_3)$, 71807-13-1; FePc(CO)(THF), 71744-41-7; FePc, 132-16-1.

Contribution from the Department of Chemistry, Oregon State University, Corvallis, Oregon 97331, School of Chemical Sciences, University of Illinois, Urbana, Illinois 61801, and Department of Chemistry, University of Arizona, Tucson, Arizona 85724

Mössbauer Effect and Magnetic Investigation of the $S = {}^3/_2 \leftrightarrow S = {}^1/_2$ Spin Crossover in [Fe(salen)NO] and the $S = {}^3/_2$ State in [Fe(5-Cl-salen)NO]

F. V. WELLS, S. W. McCANN, H. H. WICKMAN,* S. L. KESSEL, D. N. HENDRICKSON, and R. D. FELTHAM

Received April 9, 1981

The magnetic properties of quartet or doublet electronic ground states of the iron Schiff base complex [*N*,*N*′-ethylenebis(salicylideniminato)]iron nitrosyl and its 5-chloro derivative have been studied by Mössbauer, magnetic susceptibility, and EPR methods with sample temperatures in the range 4–300 K. Near 175 K, the Mössbauer spectra of [Fe(salen)NO] clearly reflect the $S = {}^3/_2 \leftrightarrow S = {}^1/_2$ transition detected by susceptibility studies reported previously by Earnshaw et al. Fluctuation rates between the two states are slow on the Mössbauer time scale, and a superposition of two spectra is seen near $T_c = 175 \pm 3$ K. The high-temperature, intermediate-spin rate state has $\Delta E_Q = 0.352 \pm 0.003$ and $\delta E = 0.440 \pm 0.003$ mm/s at 275 K. The low-temperature, low-spin state has $\Delta E_Q = 1.950 \pm 0.005$ and $\delta E = 0.281 \pm 0.001$ mm/s at 4.2 K. The Mössbauer pattern of intermediate-spin [Fe(5-Cl-salen)NO] is a slightly asymmetric quadrupole doublet at all temperatures. At 77 K, the parameters are $\Delta E_Q = 0.575 \pm 0.003$ and $\delta E = 0.654 \pm 0.003$ mm/s. Intermediate-spin states of polycrystalline samples of [Fe(salen)NO] or its derivative show broad EPR spectra corresponding to a range of g factors from ~4 to ~2. These values are consistent with Kramers levels from an $S = {}^3/_2$ term. The low-temerature $S = {}^1/_2$ state of [Fe(salen)NO] is characterized by an axial **g** tensor with $g_\perp = 2.036 \pm 0.001$ and $g_\parallel = 2.133 \pm 0.001$. At the lowest temperatures available, $T \leq 10$ K, the effective moment of [Fe(salen)NO] decreased sharply from the low-spin value. Also, in [Fe(5-Cl-salen)NO], the moment decreased from ~4 μ_B for $T \geq 120$ K to ~1 μ_B at 4 K. These results, together with Mössbauer data, are consistent with short range antiferromagnetic interactions in these lattices.

The magnetic properties of the mononitrosyl adduct of [*N*,*N*′-ethylenebis(salicylideniminato)]iron(II) are of interest because this material exhibits a relatively rare $S = {}^3/_2 \leftrightarrow S = {}^1/_2$ spin crossover near 175 K.[1,2] This property was originally reported by Earnshaw and co-workers,[1] who also showed that the crossover is modulated by substitution in the salen macrocycle. The earlier studies reported susceptibility data above 80 K, but a detailed magnetic study of this material, including Mössbauer resonance and EPR properties, has been lacking and is the subject of this report.

As is typical of transition-metal complexes displaying spin-crossover phenomena, the higher spin state (with larger atomic volume) is favored at high temperatures. Thus [Fe(salen)NO] has an intermediate spin, $S = {}^3/_2$, state above 175 K and is characterized by an $S = {}^1/_2$ state below this temperature. The transition occurs over a temperature interval of a few degrees at most. By contrast, the 5-Cl derivative retains a moment characteristic of the $S = {}^3/_2$ state at all temperatures above 50 K and below this shows evidence of antiferromagnetic interactions.

The X-ray crystal structure of [Fe(salen)NO] at 98 and 296 K has recently been reported.[3] This work has shown only marginally significant structural changes above and below the transition temperature. Both forms have a disordered nitrosyl group, and the FeNO group has a bent geometry. The average Fe–N–O angle is 147° above the transition and 127° below the transition. At the latter temperature, the iron atom is

* To whom correspondence should be addressed at Oregon State University.

(1) Earnshaw, A.; King, E. A.; Larkworthy, L. F. *Chem. Commun.* **1965**, 180.
(2) Earnshaw, A.; King, E. A.; Larkworthy, L. F. *J. Chem. Soc. A* **1969**, 2459–2463.
(3) Haller, K. J.; Johnson, P. L.; Feltham, R. D.; Enemark, J. H.; Ferraro, J. R.; Basile, L. J. *Inorg. Chim. Acta* **1979**, *33*, 119–130.

0020-1669/82/1321-2306$01.25/0

approximately 0.1 Å closer to the mean coordination plane of the salen ligand, consistent with a smaller atomic volume for the $S = {}^1/_2$ state. The fact that the NO group is disordered raises the possibility that fluctuations between atomic positions may occur on time scales affecting the Mössbauer or EPR spectra. We discuss this point and show that available data are insufficient to resolve this motion in an unambiguous fashion. The data do show, however, that the interconversion rate between $S = {}^3/_4$ and $S = {}^1/_2$ is slow on the Mössbauer effect time scale. Spectra corresponding to both spin states are observed over the temperature interval where the moment decreases from nearly 4.0 to 2.8 μ_B. This behavior may be contrasted with the situation in a related nitrosyl complex of iron tetramethylcyclam,[4] where an $S = {}^3/_2 \leftrightarrow S = {}^1/_2$ spin transition occurs on a time scale fast compared to Mössbauer frequencies. A further comparison of properties of these two systems is given in the Discussion.

Experimental Section

Compound Preparation. All reactions were accomplished in Schlenk apparatus under an atmosphere of purified argon. Argon was scrubbed of O_2 by MnO columns and then passed through 4-Å sieves to minimize the water content.[5] After the prepared complexes had been dried, they were stored in a Vacuum Atmospheres Corp. Dri-Lab glovebox equipped with an HE 493 Dri-Train.

Dimethylformamide (DMF) was shaken over KOH for 1 h, refluxed over BaO for 30 min, and fractionally distilled under argon. The center cut (10–90%) was further distilled in vacuo. Absolute ethanol was refluxed over magnesium ethoxide for 12 h and fractionally distilled under argon. All solvents used in compound preparation were degassed in vacuo. All analytical data were obtained at the Microanalytical Laboratory, School of Chemical Sciences, University of Illinois.

$Fe(C_2H_3O_2)_2 \cdot 2H_2O$ was prepared as described in the literature, by reacting reagent grade Fe wire (Mallinckrodt, 99.89%) with deionized H_2O and glacial acetic acid.[6] The Fe wire (25.0 g, 0.45 mol) was placed in H_2O (100 mL) and glacial acetic acid (150 mL) and heated to reflux for 12 h before being filtered. The green filtrate was evaporated almost to dryness, filtered, washed with reagent grade acetone (200 mL), and dried in vacuo 2 h. Analytical data indicated the ferrous acetate to be a dihydrate.

Fe^{II}(salen). The parent salen ligand was prepared as described by Martell et al.[7] by reacting salicylaldehyde with ethylenediamine in 95% ethanol. The ferrous Schiff base was prepared essentially via the method of Calderazzo et al.,[8] $Fe(CO)_5$ (3.70 mL, 27.5 mmol), which had been freshly distilled and degassed under argon, was syringed into a solution of salen (7.38 g, 27.5 mmol) in DMF (135 mL). The reaction mixture was stirred and heated to 110 °C for $2^1/_2$ h on an oil bath. The temperature was then reduced to 95 °C and maintained for 20 h. Filtration of the mixture afforded red-purple microcrystals, which were washed with DMP (20 mL) and toluene (100 mL), and dried in vacuo at 100 °C for 2 h. Anal. Calcd for Fe(salen), $C_{16}H_{14}N_2FeO_2$: C, 59.66; H, 4.38; N, 8.69; Fe, 17.34. Found: C, 59.33; H, 4.48; N, 8.89; Fe, 17.06.

Fe^{II}(5-Cl-salen)·EtOH. The Schiff base was prepared by reacting 5-chlorosalicyclaldehyde with ethylenediamine.[7] Fe^{II}(5-Cl-salen) was prepared from $Fe(C_2H_3O_2)_2 \cdot 2H_2O$ and 5-Cl-salen by a modification of a literature method.[9] $Fe(C_2H_3O_2)_2 \cdot 2H_2O$ (1.88 g, 8.95 mmol) was dissolved in deionized H_2O (20 mL) and diluted with 95% EtOH (80 mL). 5-Cl-salen (3.02 g, 8.95 mmol) and KOH (1.0 g, 17.8 mmol) were dissolved in 95% EtOH (200 mL), heated to reflux, and slowly added with rapid stirring to the $Fe(C_2H_3O_2)_2 \cdot 2H_2O$ solution. The resulting mixture was stirred for 2 h without heating before being filtered. The red-brown crystals which had formed were washed with absolute EtOH (30 mL) and dried in vacuo for 2 h.

Anal. Calcd for Fe(5-Cl-salen)·EtOH, $C_{18}H_{18}N_2FeO_3$: C, 49.46; H, 4.15; N, 6.41; Cl, 16.22; Fe, 12.78. Found: C, 49.66; H, 4.14; N, 6.40; Cl, 16.83; Fe, 12.83.

Fe(salen)NO and Fe(5-Cl-salen)NO. The nitrosyl complexes were prepared according to Larkworthy et al.[10] Thus, Fe(salen) (2.00 g, 6.21 mmol) was suspended in 95% EtOH (100 mL). Nitric oxide, purified by passing through KOH pellets, was gently bubbled through the well-stirred reaction mixture for 2 h. The black microcrystalline product was filtered, washed with 95% EtOH (30 mL), and dried in vacuo for $1^1/_2$ h. Fe(5-Cl-salen)NO was synthesized in similar fashion.

Anal. Calcd for Fe(salen)NO, $C_{16}H_{14}N_2FeO_3$: C, 54.87; H, 4.01; N, 11.93; Fe, 15.86. Found: C, 54.82; H, 4.00; N, 11.99; Fe, 15.65.

Anal. Calcd for Fe(5-Cl-salen)NO, $C_{16}H_{12}N_2Cl_2FeO_3$: C, 45.64; H, 2.87; N, 9.98; Cl, 16.84; Fe, 13.26. Found: C, 45.87; H, 3.15; N, 9.80; Cl, 16.76; Fe, 13.00.

Physical Measurements. Infrared spectra, obtained from samples prepared under argon as Nujol mulls, were recorded on a Perkin-Elmer Model 457 spectrophotometer. Variable-temperature (4.2–286 K) magnetic susceptibility data were obtained with a Princeton Applied Research Model 150A vibrating-sample magnetometer, which was operated at 13.5 kG. A calibrated GaAs temperature-sensitive diode was employed to monitor the temperature in conjunction with a $CuSO_4 \cdot 5H_2O$ standard. Electron paramagnetic resonance spectra were recorded on a Varian E-9 X-band spectrometer employing an E101 microwave bridge with a 6-in (10 kG) magnet. A Varian V-4540 variable-temperature controller was used to control the EPR sample temperature.

The Mössbauer spectrometer was of the constant-acceleration type. The source was ^{57}Co diffused in rhodium. All isomer shifts are given relative to natural iron foil at 300 K. The source was mounted on a LVsyn-loudspeaker system driven by a digitally controlled function generator with a standard feedback loop. The radiation was detected with a proportional counter and data stored in a multichannel analyzer. The sample holder was a two piece, 2.22-cm diameter lucite disk with sample area 2 cm^2 and thickness 1.0 mm. The lucite holder was sandwiched between two 0.025-cm thick low iron beryllium disks and mounted in a variable-temperature probe (heater, Si diode, and platinum sensors) which was used in a Janis Vari-Temp Dewar.

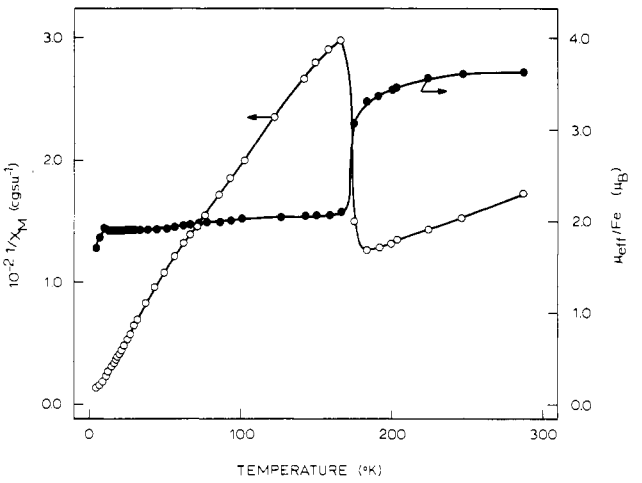

Figure 1. Magnetic susceptibility of [Fe(salen)NO] for the temperature range 4–300 K.

Data Analysis

Magnetic Susceptibility. The data for polycrystalline [Fe(salen)NO] are shown in Figure 1. These results agree with earlier studies of Earnshaw[1,2] and show clearly the spin crossover that occurs near 175 K. Above this temperature, T_c, the effective moment μ_{eff} is approximately 3.6 μ_B and below T_c it is close to 2.0 μ_B. These values are consistent with $S = {}^3/_2$ and $S = {}^1/_2$ spin states for the [Fe(salen)NO]. For sim-

(4) Hodges, K. D.; Wollmann, R. G.; Kessel, S. L.; Hendrickson, D. N.; Van Derveer, D. G.; Barefield, E. K. *J. Am. Chem. Soc.* **1979**, *101*, 906–917.
(5) Brown, T. L.; Dickerhoof, D. W.; Babus, D. A.; Morgan, G. L. *Rev. Sci. Instrum.* **1962**, *33*, 491–492.
(6) Rhoda, R. N.; Fraioli, A. V. *Inorg. Synth.* **1953**, *4*, 159–161.
(7) Martell, A. E.; Belford, R. L.; Calvin, M. *J. Inorg. Nucl. Chem.* **1958**, *5*, 170–181.
(8) Calderazzo, F.; Floriani, C.; Henzi, R.; L'Eplattenier, F. *J. Chem. Soc. A* **1969**, 1378–1386.
(9) Earnshaw, A.; King, E. A.; Larkworthy, L. F. *J. Chem. Soc. A* **1968**, 1048–1052.
(10) Earnshaw, A.; King, E. A.; Larkworthy, L. F. *J. Chem. Soc. A* **1969**, 2439–2463.

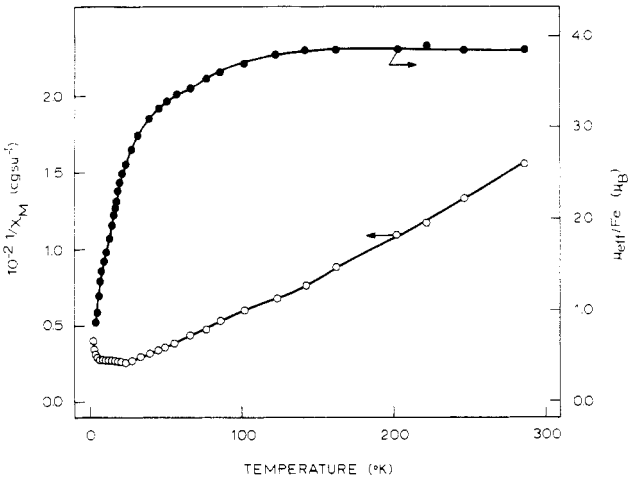

Figure 2. Magnetic susceptibility of [Fe(5-Cl-salen)NO] for the temperature range 4–300 K. Define open and closed circles.

plicity, it is convenient initially to view the magnetism of the complex as originating from orbital singlet, spin quartet, or spin doublet terms of iron(III). The high-temperature state can be denoted $^4\Gamma_H$ and the low-temperature state $^2\Gamma_L$. We later consider the orbital character of these levels and the degree of covalency present.

The magnetic behavior of [Fe(5-Cl-salen)NO], shown in Figure 2, is quite different from that of the parent complex. Particularly striking is the absence of a sharp spin-crossover transition. Instead, the data show a decrease in magnetic moment from 3.8 to 0.5 μ_B over a temperature interval of 100 K. This reveals the presence of antiferromagnetic interactions, since no ionic state of iron(III) has an effective moment lower than $\sim$1.5 μ_B.

Two kinds of antiferromagnetic ground states are typically seen in transition-metal complexes. In one case, the ions display long range order in a lattice network and the ground state involves polarized ions, $\langle S\rangle_{ion} \neq 0$, and magnetic hfs (hyperfine splitting) is observed in Mössbauer experiments. In the other case, typical of clusters with strong covalent interactions between ions, ground terms involve highly admixed ionic states and $\langle S\rangle_{ion} = 0$ when the cluster involves an even number of equivalent metal atoms. In the latter case, no magnetic field is observed in the Mössbauer spectra. In the case of [Fe(5-Cl-salen)NO], the absence of magnetic hfs in the Mössbauer spectra discussed below argues for magnetic dimers or clusters in this complex.

The simplest case for a dimer and in the present context would consist of levels derived from coupling of two ions with spin $S = {}^3/_2$. The resultant states have $S_T = 0$–3. It is also possible (but not likely for reasons discussed below) that a crossover transition occurs at the same time antiferromagnetic interactions become evident. In that event, the states involved would have $S = {}^1/_2$ and $S_T = 0, 1$.

The moment of [Fe(salen)NO] begins to decrease below $\sim$10 K. This is evidence for antiferromagnetic interaction in this complex also. Since $S = {}^1/_2$ here, potential interaction strengths are lower than for the $S = {}^3/_2$ situation. Therefore, in roughly similar lattices, the onset of antiferromagnetic behavior is expected to occur at lower temperatures.

EPR Spectra. Data for [Fe(salen)NO] are shown in Figure 3. Considered first are the results for higher sample temperatures where susceptibility data show a moment consistent with a spin quartet level. This level is assumed to be an orbital singlet for the salen complexes. When zero-field splittings of the spin levels within the term are small compared to Zeeman energies (0.3 cm^{-1}), a sharp EPR line near $g = 2.0$ is expected. In fact, a broad, polycrystalline absorption corresponding to effective spin $S = {}^1/_2$ g factors in the range 4–2 is observed.

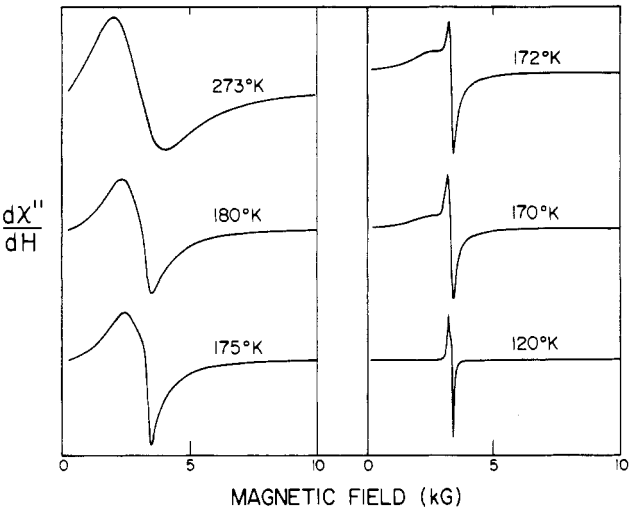

Figure 3. Polycrystalline EPR spectra for (a) [Fe(salen)NO] and (b) [Fe(4-Cl-salen)NO]. Sample temperatures are indicated.

This situation is described approximately by the usual $S = {}^3/_2$ spin Hamiltonian with $S = {}^3/_2$ and $g = 2.0$

$$\hat{\mathcal{H}} = D(\hat{S}_z^2 - \hat{S}^2) + E(\hat{S}_x^2 - \hat{S}_y^2) + g\mu_B B\cdot S \qquad (1)$$

When D is large compared to the Zeeman energy, a doublet of composition $|S = {}^3/_2, M_S \pm {}^1/_2\rangle$ has $g \simeq 2$ and $g \simeq 4$. The other Kramers doublet is nonresonant. Distributions in D and E values in individual crystallites can produce broad patterns of the type shown in Figure 3 for a sample temperature of 273 K. Single-crystal data are required to sort out the details of the line shapes and crystal field splittings.

It can be seen in Figure 3 that when [Fe(salen)NO] is cooled through the region where the sharp transition occurs in the magnetic susceptibility data, the EPR spectrum changes dramatically. The broad signal associated with the $S = {}^3/_2$ state decreases in intensity as a sharper signal at a g value of ca. 2 increases in intensity, and, finally, at temperatures below 170 K only the sharp signal is seen. The latter is attributed to the $S = {}^1/_2$ state, and it appears as an axial site symmetry EPR signal at liquid-nitrogen temperature with $g_\parallel = 2.133 \pm 0.001$ and $g_\perp = 2.036 \pm 0.001$. The spectrum does not change appreciably as [Fe(salen)NO] is cooled from 120 to 4.2 K.

The EPR spectrum of [Fe(5-Cl-salen)NO] exhibits a broad, poorly resolved signal from room to liquid-nitrogen temperature. This is consistent with the $S = {}^3/_2$ description, including exchange broadening, deduced from the susceptibility data.

Mössbauer Spectra. Representative spectra of [Fe(salen)NO] are shown in Figure 4 for a series of absorber temperatures. The solid lines are the result of curve fitting with Lorentz line shapes, as described below. The sample used in the Mössbauer work contained a small amount of iron impurity as evidenced by the quadrupole doublet with the line near 2 mm/s. The presence of the doublet did not affect the analysis of the Mössbauer data. In these experiments, the absorber was initially at 300 K and its temperature was subsequently decreased monotonically through the transition temperature T_c. When the sample temperature was increased and the measurements repeated, somewhat different spectra were observed in the region of T_c. The data showed hysteresis effects indicating that a first-order phase transition is associated with the spin-crossover transition. The hysteresis loop is displayed in Figure 5 where the absorption areas (arbitrary units) are plotted for increasing and decreasing temperature cycles. The hysteresis loop is approximately 10 K wide, and T_c is taken as 175 ± 3 K by computing the mean of the temperatures for corresponding spectra. Qualitative experi-

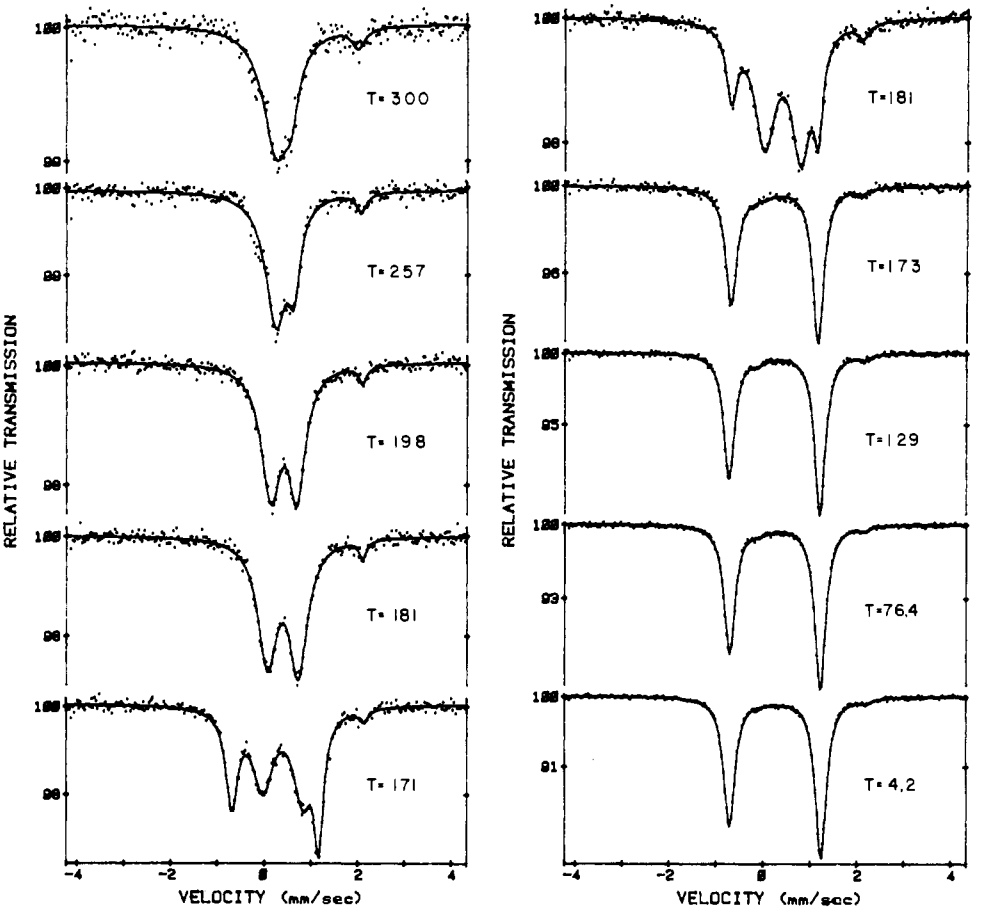

Figure 4. Mössbauer spectra for [Fe(salen)NO]. Left (right) panel corresponds to a series of measurements with decreasing (increasing) sample temperatures.

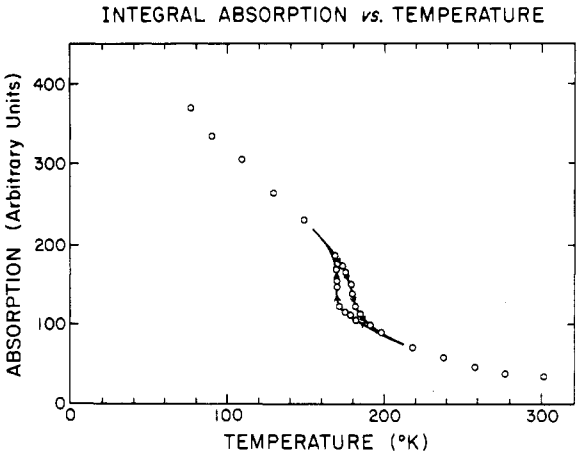

Figure 5. Mössbauer absorption area (arbitrary units) for increasing and decreasing temperature cycles.

ments on samples from different preparations showed that the width of the hysteresis loop was somewhat sample dependent in agreement with earlier work of Earnshaw et al.[2]

Figure 5 shows that the recoil free fraction, f, which we assume to be proportional to the absorption area, decreases on passing from the low-spin to the intermediate-spin state. Presumably, this decrease is associated with movement of the iron atom from an in-plane position (low-spin) to an out-of-plane position (intermediate-spin state). The latter geometry is expected to allow a larger mean nuclear displacement, $\langle R^2 \rangle$ and hence, a lower recoil free fraction. To quantify these ideas, it is necessary to deduce a lattice binding energy or Lamb–Mössbauer temperature by appropriate treatment of $f(T)$. In the present case, a detailed analysis is not possible, but we have used a simple Einstein model for the vibrational structure to estimate lattice frequencies in the low- and intermediate-spin states.

In the Einstein model, the iron motion is approximated by a local mode of frequency ω_0 which is related to the recoil free fraction by expression[11] 2, where E_γ is the Mössbauer γ-ray

$$f = \exp\left(-\left[\frac{E_\gamma^2}{2Mc^2\hbar\omega_0}\coth\frac{\hbar\omega_0}{2kt}\right]\right) \qquad (2)$$

energy, M is the atom weight of ^{57}Fe, and all other symbols have their conventional meanings. The Mössbauer data were analyzed in the following manner. Spectra at all temperatures were fit by Lorentz lineshapes by using a standard nonlinear least-squares fitting procedure. When the absorption areas are proportional to the recoil free fraction, their temperature variation can be used with eq 2 to obtain an Einstein frequency in a straightforward manner. The data used in this analysis was restricted to temperatures outside the hysteresis region. The result of the least-squares analysis of the absorption areas was

$$\hbar\omega_{LS}/k = 77 \pm 4 \text{ K} \qquad (3a)$$

and

$$\hbar\omega_{IS}/k = 64 \pm 4 \text{ K} \qquad (3b)$$

Thus, the effective Einstein frequency of the iron atom decreases by approximately 20% upon conversion from the low-spin to the intermediate-spin state. This result, as noted earlier, is consistent with a larger mean squared vibrational amplitude

(11) Wertheim, G. K. "Mössbauer Effect: Principles and Applications"; Academic Press: New York, 1964.

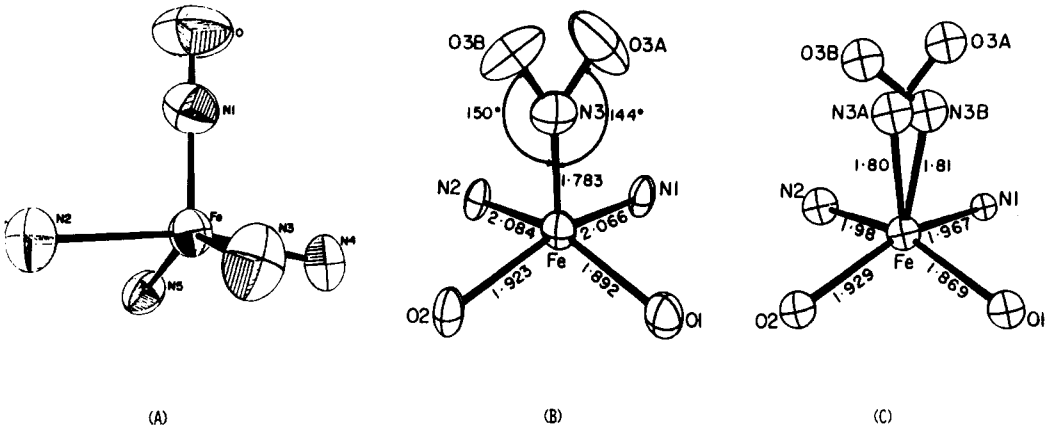

(A) (B) (C)

Figure 6. Iron coordination in spin-crossover complexes with configuration $\{FeNO\}^{+}$.

for the iron in the $S = {}^3/_2$ state.

Mössbauer spectra for the intermediate-spin region also reflect dynamic processes which produce changes in the appearance of the quadrupole pattern for temperatures above 200 K (Figure 4). There is a relatively rapid decrease in the quadrupole splitting, together with a broadening of the higher velocity component. Several sources contribute to these changes. Among these are electronic relaxation,[12,13] possible thermally activated motion of the NO group, and asymmetry in the Mössbauer recoil free fraction. However, the present data are insufficient to estimate the relative importance of these mechanisms.

The Mössbauer pattern of [Fe(5-Cl-salen)NO] consists of a simple, slightly asymmetric quadrupole doublet for $1.5 \leq T \leq 300$ K. It shows only a small increase in overall splitting as temperature is decreased. The parameters at 300, 77, and 4.2 K are respectively $\Delta E_Q = 0.537, 0.575, 0.568$ mm/s and $\delta E = 0.540, 0.653, 0.688 \pm 0.005$ m/s. At corresponding temperatures, the Mössbauer quadrupole splittings of intermediate-spin [Fe(salen)NO] and [Fe(5-Cl-salen)] are different. This suggests that the FeNO bonding, or lattice steric effects, are not identical in the two materials.

Discussion

Two classes of $\{FeNO\}^7$ complexes which exhibit $S = {}^3/_2 \leftrightarrow S = {}^1/_2$ spin-crossover behavior have now been characterized structurally. Both contain five-coordinate iron atoms with roughly square-pyramidal geometry. The first of these, $[Fe(NO)TMC]^{2+}$, where TMC = tetramethylcyclam, has a nearly linear FeNO group, a high NO stretching frequency, and coordination geometry distorted from square-pyramidal toward trigonal-bipyramidal geometry (Figure 6A).[4] These features, determined at 25 °C, are presumably also present in the low-temperature, low-spin complex. The present complex [Fe(salen)NO] has a strongly bent FeNO group, a low NO stretching frequency, and coordination sphere which is not distorted toward trigonal-bipyramidal geometry (Figure 6B,C).[3] These structural features are present in both the high- and low-temperature forms of [Fe(salen)NO]. The present study and that of Fitzsimmons et al.[14] have shown that hysteresis accompanies the spin-crossover at 175 K (Figure 5). These results, in agreement with the X-ray study,[3] indicate that a first-order structural phase transition accompanies the spin crossover.

The relationship between the structural features and electronic properties of low-spin $\{NMO\}^n$ complexes are now well established.[15-18] In Figure 7, the orbital ordering for a hypothetical linear $\{MNO\}^n$ complex with C_{4v} symmetry is set out for various ligand field strengths of the equatorial ligands. Three qualitatively different situations can be envisioned: case I in which the equatorial ligand field is weak and as a result the energy of the π^*(NO) orbital is greater than the energies of both σ^* orbitals, d_{z^2} and $d_{x^2-y^2}$; case II, where π^*(NO) lies between d_{z^2} and $d_{x^2-y^2}$; case III, where π^*(NO) is lower in energy than both d_{z^2} and $d_{x^2-y^2}$, corresponding to a strong equatorial ligand field. As was noted by Hodges et al.,[4] TMC is a weak field ligand corresponding to case I of Figure 7. Consequently, the quartet state for the hypothetical $[Fe(TMC)NO]^{2+}$ complex with C_{4v} symmetry would have the electron configuration $(d_{xz})^2(d_{yz})^2(d_{xy})^1(d_{z^2})^1(d_{x^2-y^2})^1$. This configuration would leave the π^*(NO) group orbitals unoccupied, the d_{xz}, d_{yz} orbitals filled, and hence the FeNO group should be linear.[16] However, both of the σ^* orbitals d_{z^2} and $d_{x^2-y^2}$ are occupied, leading to distortion from square-pyramidal geometry toward trigonal-bipyramidal geometry as noted earlier.[4] The result is to lower the symmetry to C_{2v} without bending the FeNO group producing the structure in Figure 6A. The low-spin form of $[Fe(TMC)NO]^{2+}$ then has the electron configuration $(d_{xz})^2(d_{yz})^2(d_{xy})^2(d_{z^2})^1$, corresponding to a linear FeNO group similar to that of $[Fe(DMDTC)_2NO]$,[19] where DMDTC = dimethyldithiocarbamate.

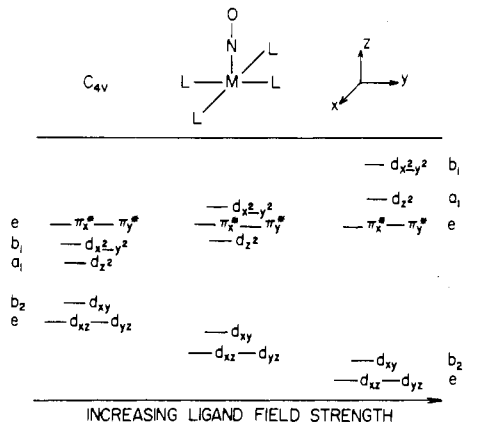

Figure 7. Qualitative orbitals for a $\{MNO\}^n$ complex with C_{4v} symmetry and increasing equatorial ligand field strengths.

(12) Blume, M. *Phys. Rev. Lett.* **1967**, *18*, 305–308.
(13) Wickman, H. H.; Wagner, C. F. *J. Chem. Phys.* **1969**, *51*, 435–444.
(14) Fitzsimmons, B. W.; Larkworthy, L. F.; Rogers, K. A. *Inorg. Chim. Acta* **1980**, *44*, 153–154.
(15) Mingos, D. M. P. *Inorg. Chem.* **1973**, *12*, 1209–1211.
(16) Enemark, J. H.; Feltham, R. D. *Coord. Chem. Rev.* **1974**, *13*, 339–406.
(17) Hoffman, R. M.; Chem, M. L.; Elian, M.; Rossi, A. R.; Mingoes, D. M. P. *Inorg. Chem.* **1974**, *13*, 2666–2675.
(18) Hawkins, T. W.; Hall, M. B. *Inorg. Chem.* **1980**, *19*, 1735–1739.
(19) Feltham, R. D.; Crain, H. *Inorg. Chim. Acta* **1980**, *40*, 37–42.
(20) Kopf, J.; Schmidt, J. *Z. Naturforsch., B: Anorg. Chem., Org. Chem.* **1977**, *32B*, 275–280, Schmidt, J.; Kuhr, H.; Dorn, W. L.; Kopf, J. *Inorg. Nucl. Chem. Lett.* **1974**, *10*, 55–61.

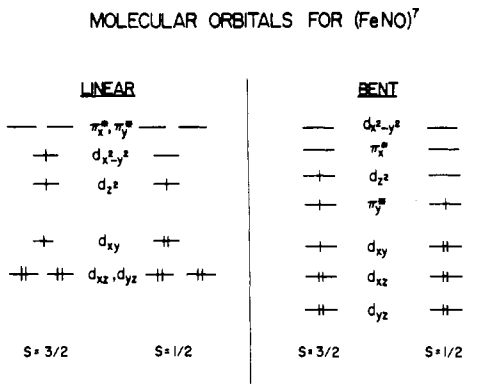

Figure 8. Schematic orbital levels for $S = {}^3/_2$ and $S = {}^1/_2$ iron nitrosyl complexes.

In contrast to the TMC complex, the properties of [Fe(salen)NO] suggest strongly that it corresponds to case II or case II of Figure 7. The fact that both high-spin and low-spin forms of [Fe(salen)NO] have strongly bent FeNO groups indicate that one component of π^*(NO) is occupied, while the fact that the square-planar array of the salen ligand is *not* distorted toward trigonal-bipyramid geometry indicates that $d_{x^2-y^2}$ is not occupied in either spin state. Based on the molecular orbital scheme of Mingos,[15] Fitzsimmons et al.[14] proposed the electronic configurations $(d_{yz}, \pi^*(NO)^2$, $(d_{xz}, \pi^*(NO))^2$, $(d_{xy})^1$, $(\pi^*NO), d_{z^2})^1$, $(\pi^*(NO), d_{yz})^1$ and $(d_{yz}, \pi^*(NO))^2$, $(d_{xy}, \pi^*(NO))^2$, $(d_{xy})^2$, $(d_{z^2})^1$ for the $S = {}^3/_2$ and $S = {}^1/_2$ states, respectively. In their proposed electron configurations for the $S = {}^1/_2$ state, the unpaired electron resides in the d_{z^2} orbital while the π^*(NO) antibonding orbitals are empty. As pointed out elsewhere,[16] such an electron configuration for an $\{FeNO\}^7$ complex would be expected to have linear FeNO geometry rather than the strongly bent geometry which is observed for the [Fe(salen)NO] complex. Moreover, the EPR spectra of $[Fe(DMDTC)_2NO]$ which does have linear FeNO geometry indicate that it has a $^2A_1$ ground state with the unpaired electron in the d_{z^2} orbital.[19] In Figure 7, the orbital ordering for case II or case III corresponds to the electron configuration for the quartet state of [Fe(salen)NO], proposed by Fitzsimmons et al., provided the separation between d_{x^2} and π(NO) is not too large. Such an electron configuration places one of the three unpaired electrons in the π^*(NO) orbitals, which corresponds to the observed bent geometry in the quartet form of [Fe(salen)NO]. Since the $d_{x^2-y^2}$ orbital is not occupied, there should be no tendency for Fe(NO)salen to distort toward trigonal-bipyramidial geometry.

The $S = {}^1/_2$ state of [Fe(salen)NO] has a bent FeNO geometry which indicates that case III of Figure 7 is the most reasonable one for a hypothetical linear complex. This would become more stable by bending the FeNO group producing a $^2A''$ ground state.[16] The molecular orbital diagrams for both high-spin and low-spin forms of $[Fe(TMC)NO]^{2+}$ and [Fe(salen)NO] are summarized in Figure 8. Except for the electron configuration of the $S = {}^1/_2$ state of [Fe(salen)NO], these molecular orbital diagrams and electron configurations are in substantial agreement with the structural features and molecular orbital description previously proposed.

The observed effect on the Mössbauer spectra in [Fe(salen)NO] can also be rationalized with the orbital scheme of Figure 8. The result of the transfer of electron density from a σ^* orbital, d_{z^2}, in the quartet state to an orbital with substantially greater d character, d_{xy}, will increase the valence contribution to the electric field gradient in the low-temperature form. At the same time, shielding of s-type iron electrons is increased leading to a larger isomer shift for the low-temperature complex. Both expectations are consistent with the [Fe(salen)NO] Mössbauer parameters for the two spin states. The foregoing orbital model is consistent with the experimental data, but the actual situation is certainly more complex. The low symmetry of [Fe(salen)NO] and the close spacing of the orbitals ensures that the levels are highly mixed, and their exact composition will be highly dependent upon the detailed structures of the high- and low-temperature forms.

It is interesting that the EFG (electron field gradient) in [Fe(5-Cl-salen)NO] is some 50% larger than in the parent complex. This is further indication that orbital composition and level spacing is a sensitive function of the FeNO geometry. It should also be noted that unlike [Fe(salen)NO], the EFG of the 5-chloro derivative (which has $S = {}^3/_2$) shows little temperature dependence. In addition, the susceptibility data indicate antiferromagnetic interactions between the complexes. Together, these results suggest that the 5-chloro complexes are arranged differently in the lattice so far as their FeNO groups are concerned. It is possible that the 5-chloro derivative involves dimers in its lattice. In turn, this may argue for a more rigid FeNO geometry and less prospect for a structural phase change and spin crossover. It is possible to interpret the increased ΔE_Q in the 5-chloro derivative as evidence for greater d character in the d_{xy}, π^*_y(NO), and d_{z^2} orbitals.

As mentioned earlier, the significant temperature variation of the EFG in the high-temperature phase of [Fe(salen)NO] differs from the behavior of that of [Fe(5-Cl-salen)NO]. This may arise because the former complex experiences fluxional motion associated with the FeNO group that is diminished in the latter compound.

In conclusion, we note that the EFG observed in the salen type $S = {}^3/_2$ complexes is markedly smaller than those observed in porphyrin intermediate spin states.[21,22] This may reflect the greater occupation of the π^*(NO) orbitals in moments in salen complexes. The magnetic moments in salen complexes tend to fall below the spin-only value of 3.88 μ_B expected for the quartet term and can be accounted for by admixture of the low-lying doublet state into the quartet ground state. Thus, the entire range of magnetic properties and Mösbauer spectra of the salen complexes can be accommodated without reference to the $S = {}^5/_2$ state. This seems reasonable since the $S = {}^5/_2$ term requires occupation of three antibonding orbitals and is therefore expected to be at energies significantly higher than the doublet or quartet states.

Acknowledgment. This research was sponsored by NSF Grant DMR 78-08452 at Oregon State University (H.H.W.), NIH Grant GM 16627 at the University of Arizona (R.D.F.), NIH Grant HL 13652 at the University of Illinois (D.N.H.), and a grant from the OSU Computer Center.

Registry No. Fe(salen)NO, 14896-33-4; Fe(5-Cl-salen)NO, 80954-24-1; Fe(5-Cl-salen), 19707-02-9.

(21) Dolphin, D. H.; Sams, J. R.; Tsin, T. B. *Inorg. Chem.* **1977**, *16*, 711–713.
(22) Reed, C. A.; Mashiko, T.; Bentley, S. P.; Kastner, M. E.; Scheidt, W. R.; Spartalian, K.; Lang, G. *J. Am. Chem. Soc.* **1979**, *101*, 2948–2958.